Preprint
UCRL-JC-147008

Imaging Collagen Orientation Using Polarization-Modulated Second Harmonic Generation

P. Stoller, P.M. Celliers, K.M. Reiser, A.M. Rubenchik

This article was submitted to
Photonics West 2002, San Jose, California, January 19-25, 2002

U.S. Department of Energy

Lawrence
Livermore
National
Laboratory

January 10, 2001

DISCLAIMER

Imaging collagen orientation using polarization-modulated second harmonic generation

Patrick Stoller*[a], Peter M. Celliers[a], Karen M. Reiser[b], Alexander M. Rubenchik[a]

[a]Medical Technology Program, Lawrence Livermore National Laboratory;
[b]Department of Neurosurgery, University of California, Davis

ABSTRACT

We use polarization-modulated second harmonic generation to image fiber orientation in collagen tissues, with an axial resolution of about 10 μm and a transverse resolution of up to 1 μm. A linearly polarized ultra-short pulse (200 fs) Ti:Sapphire laser beam is modulated using an electro-optic modulator and quarter-wave plate combination and focused onto a translation stage mounted sample using a microscope objective. The generated second harmonic light is collected using a photomultiplier tube and demodulated using phase sensitive detection to obtain signal intensity and fiber orientation information. In order to obtain second harmonic generation images of different types of collagen organization, we analyze several different tissues, including rat-tail tendon, mouse aorta, mouse fibrotic liver, and porcine skin. We can use our technique to image fibrotic tissue in histological sections of damaged liver and to identify burned tissue in porcine skin to a depth of a few hundred microns. Polarization-modulated second harmonic generation potentially could be a useful clinical technique for diagnosing collagen related disease or damage, especially in the skin.

Keywords: second harmonic generation, polarization, ultra-short pulse laser, scanning microscopy, collagen, rat-tail tendon, liver fibrosis, knee cartilage, porcine skin

1. INTRODUCTION

Collagen is the most abundant structural protein in the body. It is found, to mention only a few examples, in tendon, ligament, bone, fascia, arterial wall, and cornea. There are more than twenty genetically distinct types of collagen, but the different types can generally be classified as either fibrillar or non-fibrillar. In this work, we focus on the fibrillar collagens, especially Type I collagen. Fibrillar collagen molecules are typically triple-helical structures; they organize into long, narrow fibrils with a length on the order of microns and a diameter between 5 nm and 500 nm. These fibrils are themselves often organized into macroscopic bundles called fibers. Collagen fibers have diameters on the order of a few microns. The high degree of organization found in collagen—from the molecular to the macroscopic level—coupled with the absence of inversion symmetry in the structure allows second harmonic generation (SHG) in the presence of high electric fields, such as those present in intense laser light. The absence of organization on the scale of the wavelength of light would prevent significant SHG.

Why should we be interested in second harmonic generation in collagen? Numerous disease states, including abnormal wound healing, skin cancer, diabetes, osteoarthritis, and liver fibrosis are related to changes in collagen structure. For many of these conditions, there are characteristic, early changes in the organization of the collagen that could potentially serve as an early diagnostic marker. Early changes in collagen structure haven been observed in samples analyzed using electron microscopy[1], x-ray diffraction[2], biochemical analysis, histological analysis, and physiological assessment. A major drawback of these techniques is that they are often destructive and can only be done on samples obtained through tissue biopsy. In many cases it may not be feasible to obtain a tissue biopsy for diagnostic screening, nor may it be

* stoller2@llnl.gov; phone 1-916-734-0833; fax 1-925-424-2778; Lawrence Livermore National Laboratory; L-174, P.O. Box 808, Livermore, CA 94551

practical to monitor treatment with sequential biopsies. Second harmonic generation microscopy could be applied to non-invasive imaging of collagen, especially in the skin.

Second harmonic generation was first observed in biological tissue in 1971[3]. Several other studies of SHG in different tissues, including rat-tail tendon, cornea, and teeth, followed[4-12]. The advent of the ultra-short pulse laser, which permitted the necessary high intensity for SHG without depositing too much energy in the tissue, allowed SHG microscopy to be performed in biological tissue without damaging the sample[13-18]. Previous work[5-7], as well as our own recent studies[19], suggest that measuring the polarization dependence of the SHG provides more information than the intensity alone. The polarization dependence of the SHG signal gives information about the orientation and nonlinear susceptibility tensor of the collagen fibers. Direct measurement of the polarization dependence, however, is time consuming as it requires repeated measurement of the SHG signal at a single point in the sample. We have developed a polarization-modulation technique that allows fiber orientation to be measured rapidly[20,21]. Here we apply this technique to orientation imaging in several new tissues, including mouse artery, fibrotic liver, and porcine skin.

2. EXPERIMENT

2.1 Optical setup

We used a Ti:Sapphire ultra-short pulse laser (Coherent Mira) to generate 200 fs pulses of linearly polarized light with wavelength centered at 800 nm, maximum energy per pulse 5 nJ, and repetition rate 76 MHz. The laser beam was first passed through a half-wave plate and a polarizing beam-splitter; the half-wave plate was rotated to control the power incident on the sample. The p-polarized light was then rotated 45 degrees using a second half-wave plate. The beam then passed through an electro-optic modulator (Conoptics 360-80) with its fast and slow axes oriented at 45 degrees to the polarization of the incident light. The beam was spatially filtered and expanded and, after it reflected off of several dielectric mirrors, it was passed through a quarter-wave plate with its fast and slow axes oriented at 45 degrees to those of the electro-optic modulator. After reflecting off of a dichroic mirror, the beam was focused onto the translation stage mounted sample using a microscope objective (Mitutoyo infinity corrected plano-apochromat). The objective had focal length f = 1 cm, numerical aperture N.A. = 0.42, transverse resolution around 1.5 μm, and axial resolution around 10 μm. Transmitted second harmonic light was collected using a second microscope objective and detected using a photomultiplier tube. Back-scattered second harmonic light was collected by the same objective used to focus the laser beam onto the sample, transmitted through the dichroic mirror, and collected using a second photomultiplier tube. This experimental setup is illustrated in Figure 1 below.

2.2 Polarization-modulation

The electro-optic modulator and quarter-wave plate combination were used to rotate the direction of the polarization of the linearly polarized laser beam. An electro-optic modulator is equivalent to a variable wave plate; the phase delay is proportional to the voltage applied across it. For linearly polarized input light, the electro-optic modulator produces elliptically polarized light. The quarter-wave plate that follows the electro-optic modulator converts the elliptically polarized light into linearly polarized light rotated by some angle with respect to the laser polarization direction. The degree of rotation is directly proportional to the applied voltage: from 0 degrees for 0 V to 180 degrees for the full-wave voltage of the electro-optic modulator. The voltage across the electro-optic modulator can be modulated at high frequencies; our system is limited to a bandwidth of 1 MHz.

2.3 Phase sensitive detection

A function generator provided a saw-tooth waveform at 4 kHz that was amplified to have an amplitude equal to the full-wave voltage of the modulator using a high voltage power supply (Conoptics 302A). The polarization modulated beam produces SHG in the sample that is modulated at the first and second harmonic of the modulation frequency (the origin of these modulations is discussed in *Theory*, below) After passing through a current preamplifier, the modulated signal from the PMT was amplified using two lock-in amplifiers set to detect the amplitude and phase of the SHG signal at both the first and second harmonic of the EOM modulation frequency. A Labview program was used to coordinate motion of the translation stage using a motion controller (Newport ESP300) and Newport 850F actuators and to acquire data from the lock-in amplifiers.

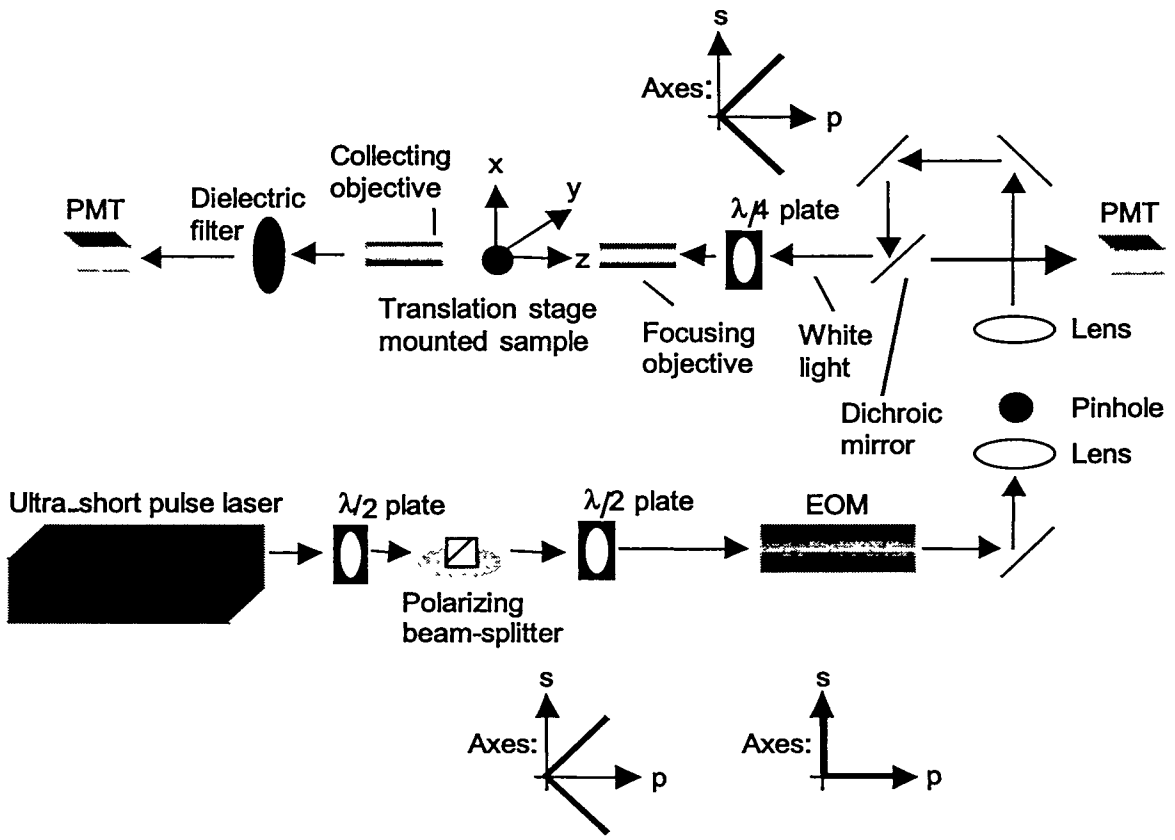

Figure 1. Illustration of the experimental setup.

2.4 Sample preparation

Rat-tail tendon from 3-4 month old Sprague-Dawley rats was frozen at –20 degrees C until scanned. We previously had found that freezing and thawing did not affect the second harmonic signal. Individual fascicles were removed from the tendon bundles under a dissecting microscope. Typical fascicles were several centimeters long, and had a diameter of only a few tenths of a millimeter. Unicryl-mounted sections of mouse aorta (5 μm thick) were a kind gift of Adam Mullick of the University of California, Davis. Paraffin-mounted sections of fibrotic liver tissue (3 to 5 μm thick) were a kind gift of Mark Zern and Jian Wu of the University of California, Davis. Sections of liver tissue were obtained from mice that had severe liver fibrosis due to the ingestion of carbon tetrachloride (CCl_4). Porcine skin was obtained from a local supermarket and stored frozen at –20 degrees C until used. The center of a 1 cm by 1 cm section of porcine skin was burned using a narrow metal rod (diameter ~1 mm) heated to 200 degrees C to simulate burn damage.

3. THEORY

The theory we use has been described in detail in previous work[21]; here, we provide only a brief summary. We use the coordinate system illustrated in Figure 2 below. The laser is incident along the z-axis, the fibril bundles are oriented at some angle ϕ from the y-axis in the x-y plane. The polarization angle of the laser beam α in the x-y plane is measured from the x-axis. We assume that the collagen fibers have cylindrical symmetry. We make the paraxial approximation

and we neglect birefringence, non-normal incidence of the beam on the sample, and polarization dependent scattering. Under these assumptions, the second harmonic signal intensity in the tissue is proportional to

$$I_{SHG} \propto \frac{1}{8}(3+20\gamma+40\gamma^2) - \frac{1}{2}(1+6\gamma+8\gamma^2)Cos(2\alpha+2\phi) + \frac{1}{8}(1+4\gamma)Cos(4\alpha+4\phi) \quad (1)$$

where γ is a parameter of the second order non-linear susceptibility tensor. Since the polarization of the input laser light is modulated in a saw-tooth pattern at a frequency Ω, we have $\alpha = \Omega t$. Substituting into Equation 1, we get

$$I_{SHG} \propto \frac{1}{8}(3+20\gamma+40\gamma^2) - \frac{1}{2}(1+6\gamma+8\gamma^2)Cos(2\pi\Omega t+2\phi) + \frac{1}{8}(1+4\gamma)Cos(4\pi\Omega t+4\phi) \quad (2)$$

It is clear from Equation 2 that the phase of the signal at the first modulation harmonic (described by the second term in the equation) is 2ϕ. Therefore, the orientation of the collagen fiber is given by half of the phase measurement.

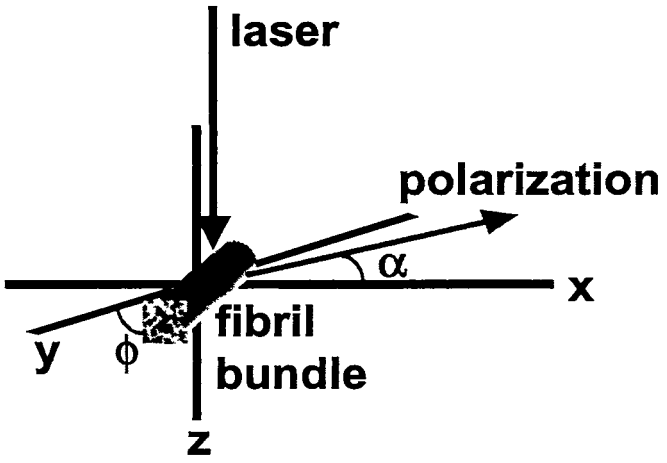

Figure 2. Sketch of the fiber orientation and laser beam propagation direction and polarization.

4. RESULTS

We imaged various tissues with different collagen structures in order to determine if our technique could distinguish between them. We first imaged fiber orientation in a section of rat-tail tendon, which exhibits a well-known, highly organized structure of parallel collagen fibers. Figure 3 shows a typical example of an image of fiber orientation in rat-tail tendon acquired using second harmonic light transmitted through the sample. At each point, a line segment indicates the direction in which the collagen fibers at that location are oriented. All line segments are drawn to equal length. Points at which no line segments are shown had second harmonic signal intensity that was below the noise threshold. The image in Figure 3 shows a scan taken near the surface of the rat-tail tendon, in a plane normal to the propagation direction of the laser beam (the x-y plane, refer back to Figure 2). We also imaged samples in a plane parallel to the propagation direction (x-z plane). Figure 4 shows an image obtained in a sample of two overlaid rat-tail tendons. The image suggests a depth resolution of about 10 μm—which corresponds to the Rayleigh range of the beam—can be achieved.

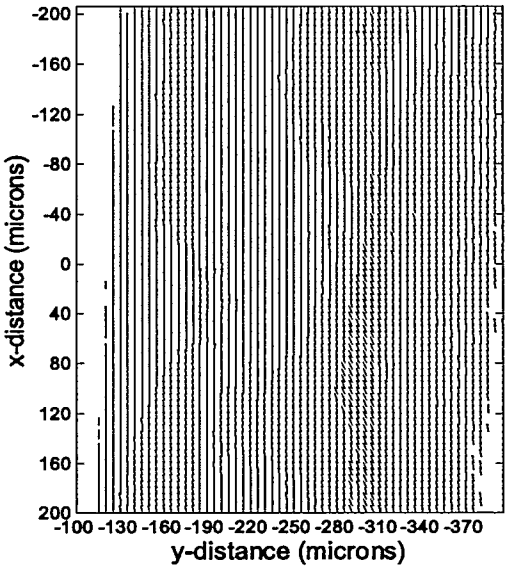

Figure 3. Orientation image of an x-y section of rat-tail tendon (fascicle aligned in the plane normal to the laser beam propagation direction). The orientation line segments indicate the very uniform fiber orientation. All segments are drawn to the same length.

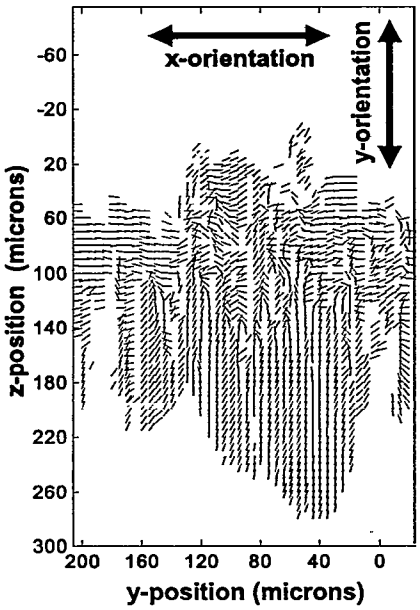

Figure 4. Orientation image of a y-z section of two overlapping rat-tail tendon fascicles (fascicles aligned in the plane normal to the laser beam propagation direction, at an angle of ~90 degrees to each other). The samples have been slightly compressed between glass slides; the two fascicles overlap between about 0 and 200 micrometers. The point $z = 0$ refers approximately to the surface of the top fascicle; depth in the fascicles increases with increasingly positive z. Note that the orientation lines in the image are not in the y-z plane; they are in the x-y plane, normal to the beam.

We next investigated several tissues with two-dimensional (in the plane normal to the laser beam) structures more complicated than that found in rat-tail tendon. The collagen fibers in the adventitia of mouse aorta are imaged in Figure 5 below. Figure 5 shows an SHG orientation scan made in a small region of a 5 micron thick cross-section of the artery. It illustrates that collagen fibers in the adventitia are organized generally tangential to the aorta cross-section, but there is considerably more disorder in the structure than in rat-tail tendon.

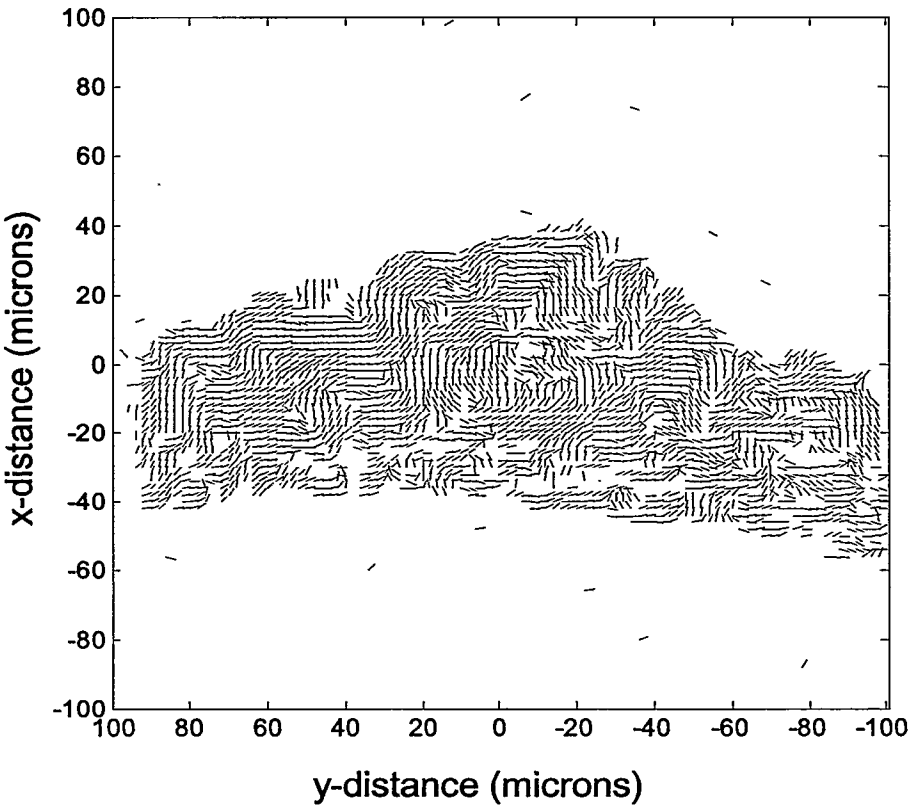

Figure 5. Orientation image of mouse aorta. The mouse aorta was sectioned normal to its axis; here, we show an image of fiber orientation in a small region of such a section. Detectable SHG signal was only observed in the adventitia.

We then studied fiber orientation in mouse fibrotic liver tissue. In Figure 6 below, we show an SHG orientation image from a section of liver showing advanced fibrosis and liver damage, obtained from a mouse exposed to carbon tetrachloride (CCl_4). Visible on the right of Figure 6 (the semi-circular pattern of line segments) is collagenous tissue surrounding the cross-section of an artery. The fibrous tissue stretching across the image to the left of the artery is fibrotic tissue not seen in images of healthy, control livers (image not shown). The collagen surrounding the artery is also considerably thicker than that observed in control samples.

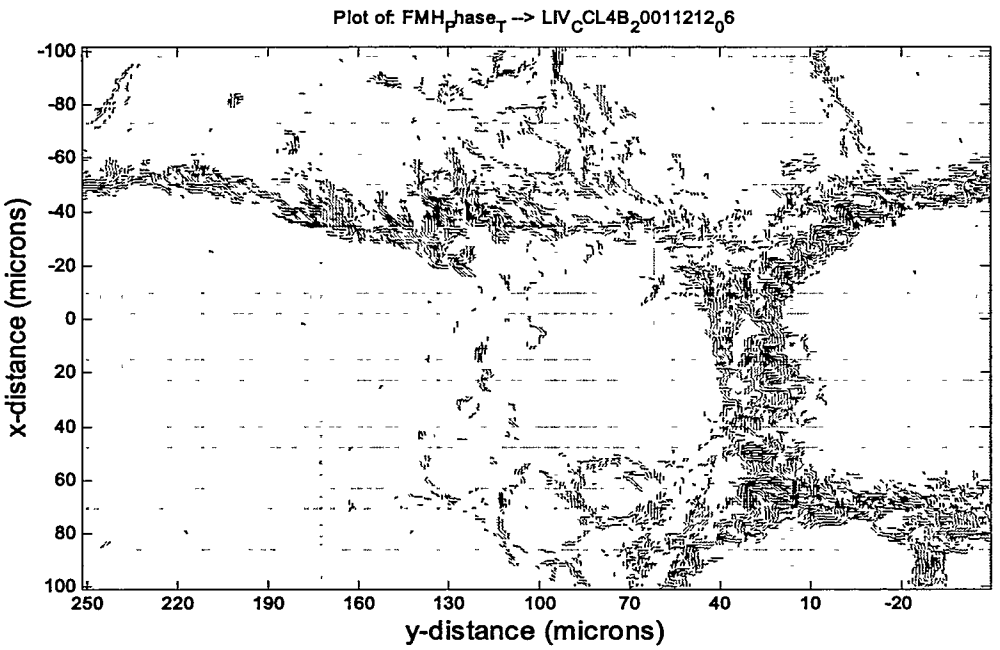

Figure 6. Orientation image of a section of mouse fibrotic liver. The image clearly shows the fibrous tissue that penetrates the liver.

We have also obtained preliminary results in porcine skin at the boundary between normal and burned tissue. In Figure 7, the burned area corresponds to the left side of the figure while the undamaged area is at the far right. Note that significant SHG is observed in the raised part of the tissue at the edge of the burn (between y = –500 μm and y = –700 μm) Unlike in the previous samples, data in this case was collected using the back-scattered component of the SHG signal; the porcine skin is too thick to allow transmitted SHG light to be collected. These first studies suggest that it is possible to obtain information about fiber orientation in the back-scattering direction, an important condition for eventual application of this technique to clinically relevant problems. The region on the left side of the figure (the burned area of the tissue) does not have any orientation lines because the SHG signal there was too low.

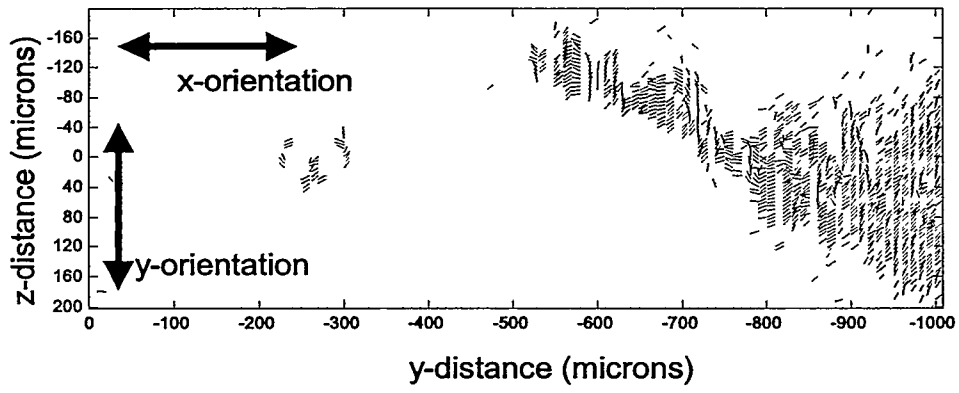

Figure 7. Orientation image of an x-z region of porcine skin at the boundary between normal and burned tissue. Note that the orientation line segments in the image are not in the y-z plane; they are in the x-y plane, normal to the beam. There are no orientation line segments on the left side of the image because the burned tissue did not produce detectable SHG.

5. CONCLUSIONS

We have demonstrated that polarization-modulated SHG is succesful in measuring collagen fiber orientation in a variety of different tissues. Experiments with highly organized rat-tail tendon—where orientation of the fibers is well known—demonstrate that it is possible to measure fiber orientation as a function of depth in tissue. We were also able to image fiber orientation in two-dimensional sections of more complex structures—such as mouse artery or fibrotic liver tissue. In fibrotic liver tissue, for instance, SHG microscopy detects collagen fibers in unstained sections that would otherwise only be visible after staining the tissue. Not only does SHG microscopy eliminate the need to stain the tissue to observe the location of collagen, but it provides direct orientation information about the fibers. Preliminary images of fiber orientation as a function of depth in porcine skin—acquired using the back-scattered component of the second harmonic signal—suggests that this technique can be applied to imaging in the axial direction to a distance of ~200 microns. More effort is needed to determine the effect of polarization dependent back scattering and other linear optical properties of the tissue on the orientation measurement. SHG microscopy has promise for imaging collagen organization in vivo; potential clinical applications include diagnosing skin cancer, burn depth and severity, and abnormal wound healing.

ACKNOWLEDGEMENTS

We thank Adam Mullick at the University of California, Davis Department of Internal Medicine: Cardiology for providing us with Unicryl mounted sections of mouse aorta. We thank Dr. Mark Zern and Dr. Jian Wu of the University of California, Davis Department of Internal Medicine for providing us with paraffin mounted sections of fibrotic mouse liver tissue. This work was supported by grants from the National Institutes of Health, 1 R01 AR 46885-01 and from the Center of Excellence for Laser Applications in Medicine, U.S. Department of Energy DE-FG03-98ER62576. This work was performed under the auspices of the U.S. Department of Energy at Lawrence Livermore National Laboratory under contract W-7405-ENG-48.

REFERENCES

1. B. Eyden and M. Tzaphlidou, "Structural variations of collagen in normal and pathological tissues: role of electron microscopy," *Micron* **32**, 287-300 (2001).
2. V. J. James, L. Delbridge, S. V. McLennan, and D. K. Yue. "Use of x-ray diffraction in study of human diabetic and aging collagen," *Diabetes* **40**, 391-394 (1991).
3. S. Fine and W. P. Hansen, "Optical second harmonic generation in biological tissues," *Applied Optics* **10**, 2350-2353 (1971).
4. M. Delfino, "A comprehensive optical second harmonic generation study of the non-centrosymmetric character of biological structures," *J. Biol. Phys.* **6**,1 05-117 (1979).
5. S. Roth and I. Freund, "Second harmonic generation in collagen," *Journal of Chemical Physics* **70**, 1637-1643 (1979).
6. S. Roth and I. Freund, "Optical second-harmonic scattering in rat-tail tendon," *Biopolymers* **20**, 1271-1290 (1981).
7. I. Freund, M. Deutsch, and A. Sprecher, "Connective tissue polarity: Optical second-harmonic microscopy, crossed-beam summation, and small-angle scattering in rat-tail tendon," *Biophysical Journal* **50**, 693-712 (1986).
8. G. B. Altshuler, N. R. Belashenkov, G. A. Martsinovski, and A. A. Solounin, "Nonlinear transmission and second-harmonic generation in dentin in the field of ultrashort ND-laser pulses," in *Advanced Laser Dentistry,* G. B. Altshuler, R. J. Blankenau, and H. A. Wigdor, eds. Proc. SPIE **1984**, 6-10 (1995).
9. E. Georgiou, T. Theodossiou, V. Hovhannisyan, K. Politopoulos, G. S. Rapti, and D. Yova, "Second and third optical harmonic generation in type I collagen, by nanosecond laser irradiation, over a broad spectral region," *Optics Communications* **176**, 253-260 (2000).
10. T. Theodossiou, E. Georgiou, V. Hovhannisyan, and D. Yova, "Visual observation of infrared laser speckle patterns at half their fundamental wavelength," *Lasers in Medicine and Surgery* **16**, 34-39 (2001).
11. V. Hovanessian and A. Lalayan, "Second harmonic generation in biofiber-containing tissue," *Proc. Int. Conf. Lasers* **96**, 107-109 (1997).
12. R. T. Bailey, F. R. Cruickshank, D. Pugh, J. N. Sherwood, and S. Wilkie, "Nonlinear optical behaviour of fish scales," *Ferroelectrics*,1 **995**, 293-299 (1995).

This work was performed under the auspices of the U.S. Department of Energy by the University of California, Lawrence Livermore National Laboratory under Contract No. W-7405-Eng-48.

13. B-M Kim, J. Eichler, and L. B. Da Silva, "Frequency doubling of ultrashort laser pulses in biological tissues," *Applied Optics* **38**, 7145-7150 (1999).
14. B-M Kim, J. Eichler, K. M. Reiser, A. M. Rubenchik, L. B. Da Silva, "Collagen Structure and Nonlinear Susceptibility: Effect of Heat, Glycation, and Enzymatic Cleavage on Second Harmonic Signal Intensity", *Lasers in Surgery and Medicine*, **27** 329-335 (2000).
15. B-M. Kim, P. Stoller, K. M. Reiser, J. Eichler, M. Yan, A. M. Rubenchik, and L. B. Da Silva, "Confocal imaging of biological tissues using second harmonic generation," *Proc. SPIE* **3914**, 435-440 (2000).
16. Y. Guo, P. P. Ho, A. Tirksliunas, F. Lui, R. R. Alfano, "Optical harmonic generation from animal tissues by the use of ps and fs laser pulses," *Applied Optics* **35**, 6810-6813 (1996).
17. Y. Guo, P. P. Ho, H. Savage, D. Harris, P. Sacks, S. Schantz, F. Liu, N. Zhadin, and R. R. Alfano, "Second-harmonic tomography of tissue," *Optics Letters* **22**, 1323-1325 (1997).
18. P. J. Campagnola, H. A. Clark, W. A. Mohler, A. Lewis, and L. M. Loew, "Second-harmonic imaging microscopy of living cells," *Journal of Biomedical Optics* **6**, 277-286 (2001).
19. P. Stoller, B-M. Kim, K.M. Reiser, A. M. Rubenchik, and L. B. Da Silva, "Polarization dependent optical second harmonic imaging of rat-tail tendon," *Journal of Biomedical Optics* (in press).
20. P. Stoller, B-M. Kim, A. M. Rubenchik, K. M. Reiser, L. B. Da Silva, "Measurement of the second order non-linear susceptibility of collagen using polarization modulation and phase-sensitive detection". *Commercial and Biomedical Applications of Ultrashort-pulse Lasers*, Proc. SPIE **4276** (2001).
21. P. Stoller, K. M. Reiser, P. M. Celliers, and A. M. Rubenchik, "Polarization-modulated second harmonic generation in collagen". submitted to *Biophysical Journal.*